Relativistic mean fields within the chiral confining model

Presented by : Mohamad CHAMSEDDINE

10/07/2025

Motivation for studying dense matter

The status of QCD dense matter

Adam Mann, 2020

- The state of matter at high densities remains a mystery (quark-gluon plasma, hyperons, color superconductivity, …)
- QCD is perturbative but above ~$40n_{sat}$!!
- No theory, only models apply in the regime of low-T and large densities.

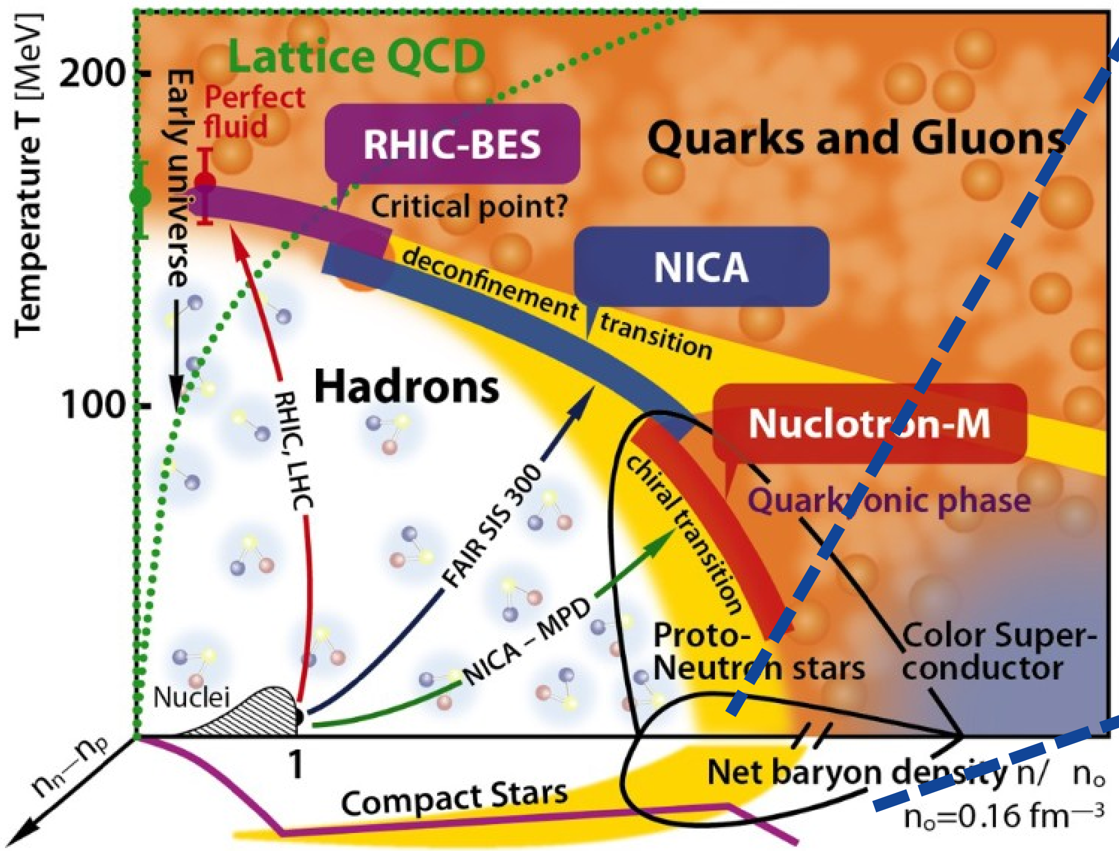

A. Yu. Kotov, 2019

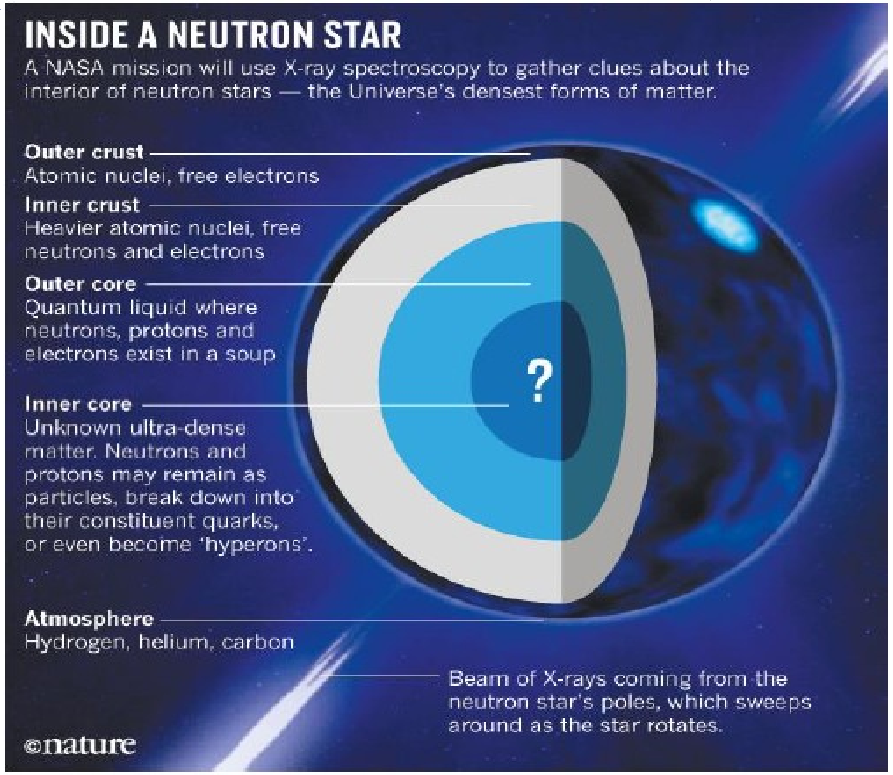

- The remnant of massive dead stars
- Densest matter in the universe: 6-8 times saturation density !
- Excellent laboratory to study dense matter
- Their core remains a mystery

NS observables

- We solve the hydrostatic equations in GR for spherical and nonrotating stars (TOV equations).
- One-to-one correspondence between EoS and M-R curve
- We can extract tidal deformabilities from gravitational waves (LIGO/VIRGO) or compactness from X-ray measurements (e.g NICER)

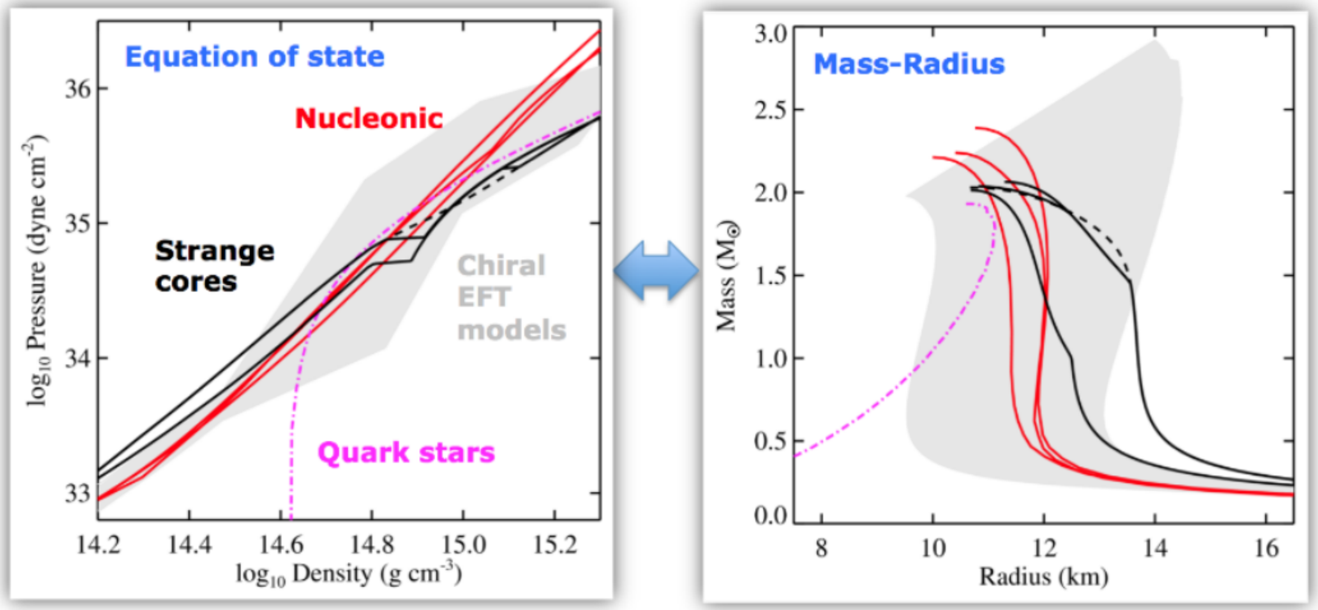

Tolman-Oppenheimer-Volkov equations

$$\frac{dp}{dr} = -\frac{G}{c^4}\frac{(mc^2 + 4\pi pr^3)(\varepsilon + p)}{r(r - 2Gm/c^2)}$$

$$\frac{dm}{dr} = 4\pi\frac{\varepsilon}{c^2}r^2$$

Motivation for relativistic models

Why relativistic models ?

Many models for nuclear matter exist, with **chiral effective theory** being one of them: a perturbative expansion in with a hierarchy of leading orders

Advantages

- A control of the uncertainty as a function of , allowing to set the limitation of the EFT

Limitations

- Breaks down at ~ 1-2n_{sat}, whereas we need to describe nuclear matter at higher densities

→ **Needs a complementary approach to describe higher densities (piecewise polytropes, sound-speed model, meta-model, etc)**

At high density, we need a **relativistic approach** since the sound speed in NS cores is expected to be larger than 10% of the light speed, as confirmed by analyses of recent radio as well as X-ray observations from NICER of massive NSs.

Advantages

- Built-in relativistic structure (spin, spin-orbit potential...) + can go beyond 2n_{sat}

Limitations

- No simple way to decide where the model breaks down, or to quantify the uncertainties.

→ **We thus employ Bayesian statistics to explore the relation between observables uncertainties and the one in the model predictions**

Aspects of the Strong Interactions

The meson exchange models

- The nuclear force is short ranged and strongly attractive at nuclear distance (0.5 – 3 fm)
- It should turn repulsive at inter-nucleon distances (hard core)
- It should have a spin dependency : tensor and spin-orbit force

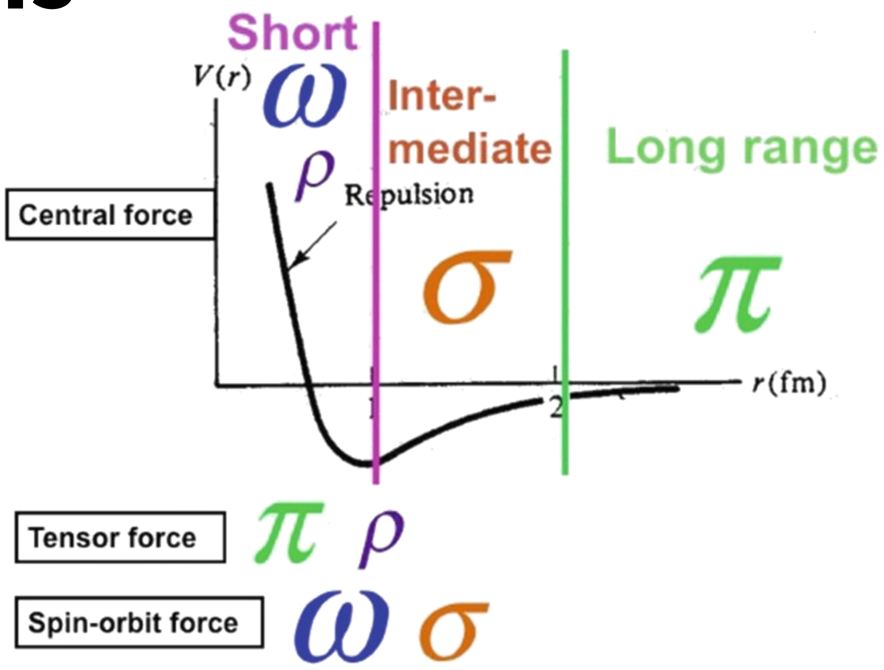

Meson	Mass (MeV)	(J^P, T)	Field	Interaction
σ	500 ??	$(0^+, 0)$	scalar-isoscalar	middle range
ω	783	$(1^-, 0)$	vector-isoscalar	short range
π	140	$(0^-, 1)$	pseudoscalar-isovector	long range
ρ	770	$(1^-, 1)$	vector-isovector	isospin part
δ	983	$(0^+, 1)$	scalar-isovector	isospin part

1) Chiral symmetry

- At the limit of zero quark masses (u,d), QCD has a chiral symmetry (non-interacting quarks with opposite parity are indistinguishable and do not couple to each other)
- Had the chiral symmetry been realised in nature, we would have observed for each meson, a partner meson with the SAME mass but opposite parity => the symmetry is broken

The radial component of the chiral field corresponds to the σ meson of Walecka, first identified by *Chanfray, Ericson, Guichon (PRC 63 (2001))*, and the phase component corresponds to the massless Goldstone boson, the pion

But since the quarks have a small mass, the symmetry is also explicitly broken and the pion acquires a small mass!

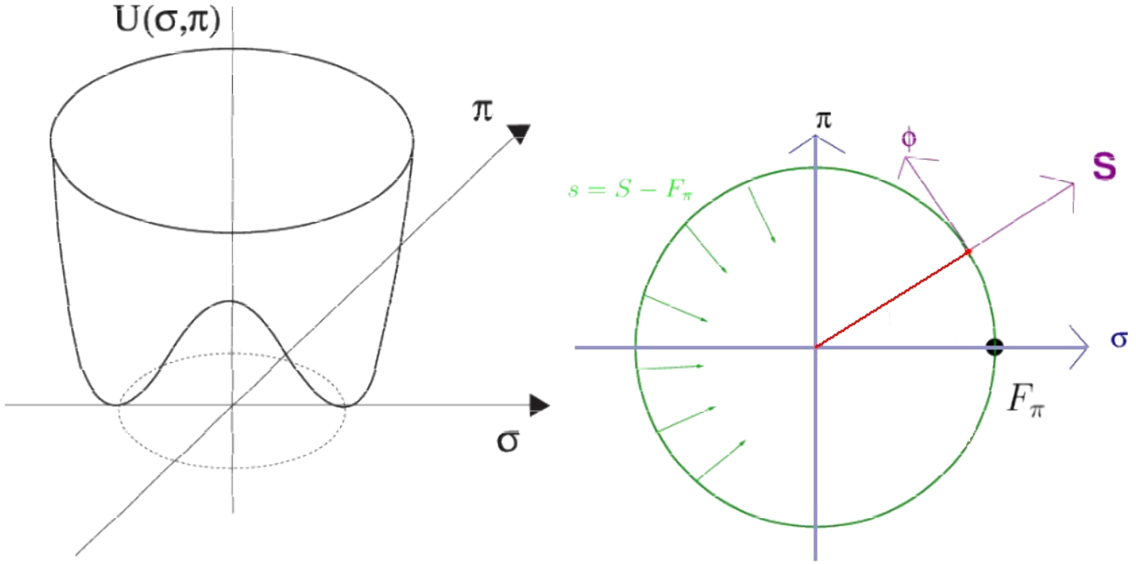

2) Confinement

- It is well established that in QCD, only colour neutral objects can be observed
- Nucleons, being made of quarks and gluons, are polarised by external fields
- In Guichon's work (*Guichon, Phys. Lett. B 200 (1988)*), the quarks wave functions get modified by the scalar field => the nucleon mass depends on the surrounding scalar field:
- We parametrize the nucleon mass as [1,2]:

$$M_N(s) = M_N + g_S\, s + \frac{1}{2}\kappa_{NS}\left(s^2 + \frac{s^3}{3\, f_\pi}\right)$$

Nucleon polarisation

The response parameters g_s and κ_{NS} might be given by an underlying confining model (for example NJL + confining potential)

[1] *Chanfray and Ericson, EPJA (2005)*
[2] *Chanfray and Ericson, PRC75 (2007)*

Motivation for relativistic models

Aspects of the Strong Interactions

The Chiral confining model

1. *Chamseddine, Margueron, Chanfray, et al. Relativistic Hartree–Fock chiral Lagrangians with confinement, nucleon finite size and short-range effects. EPJA59 (2024)*
2. *Chamseddine, Margueron, Hansen, Chanfray, Hartree-Fock Lagrangians with a Nambu-Jona–Lasino scalar potential. EPJA60 (2024)*
3. *Chanfray, EPJA (2024),*
4. *Chanfray, Ericson, Martini, Universe 9.7 (2023)*
5. *Massot, Chanfray, PRC78 (2008)*
6. *Chanfray and Ericson, PRC75 (2007)*
7. *Chanfray and Ericson, EPJA (2005)*

What is the Chiral Confining Model ?

- An effective model describing the nuclear interaction as an «exchange» of mesons.
- A lagrangian based on chiral symmetries from QCD and confinement of quarks (anchored to QCD).
- The mesons field will be decomposed as such (**RHF-CC treatment**) :

$$\varphi_R = \overline{\varphi_R} + \Delta\varphi_R$$

Classical value Hartree level

Small fluctuations Fock level

LQCD and confining models

κ_{NS}, or the dimensionless constant = (κ_{NS} $2M_N$), is expected by realistic confining potentials to **always be smaller than one** : MIT bag model, Simple models[1], QCD connected chiral confining model[2]

- It is possible to link g_s and κ_{NS} to LQCD which expresses the nucleon mass as:

$$M_N(m_\pi^2) = a_0 + a_2 m_\pi^2 + a_4 m_\pi^4 + \ldots + \Sigma_\pi(m_\pi^2, \Lambda)$$

- When using the Linear Sigma Model (LσM) for the chiral potential, we get [3]:

[1] *Chanfray and Ericson, PRC83 (2011)*
[2] *Chanfray, Ericson, Martini, Universe 9.7 (2023)*
[3] *Chanfray and Ericson, PRC75 (2007)*

Parameterisation

4 free parameters :

Tensor interaction coupling

- = 6.6 suggested by scattering data
- = 3.7 suggested by the Vector Dominance Model (VDM)
- = 0 as a reference case

Constraints	centroid	std. dev.
a_2 (GeV^{-1})	1.553	0.136
a_4 (GeV^{-3})	-0.509	0.054
E_{sat} (MeV)	-15.8	0.3
n_{sat} (fm^{-3})	0.155	0.005

LσM results

Chamseddine, M. et al EPJA59 (2024)

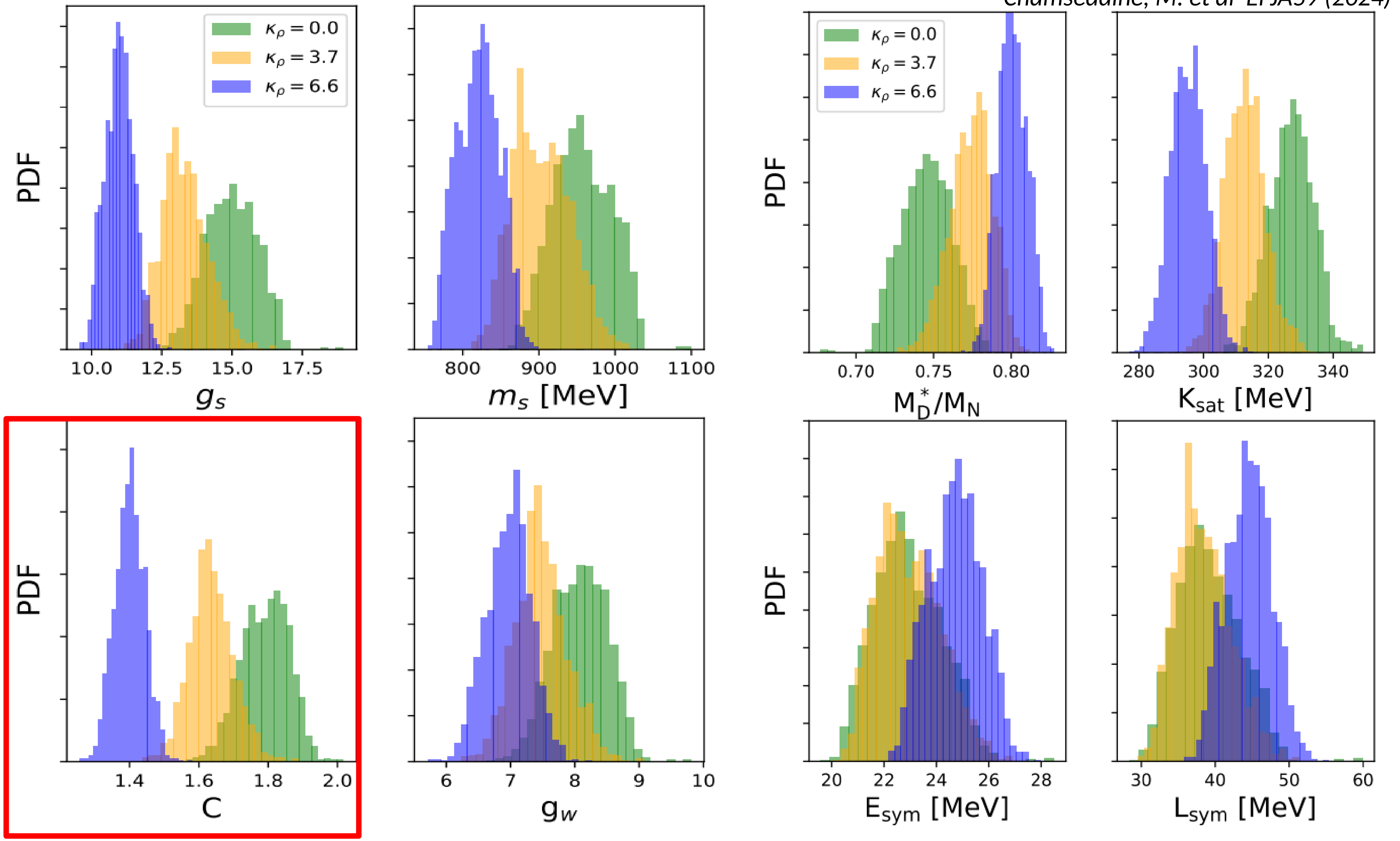

These give incompatible values with what LQCD predicts for a2 and a4

Key points

The chiral confining model is a relativistic meson exchange model incorporating the two aspects of QCD: chiral symmetry and confinement

is larger and is smaller than their experimental values

Tension between LQCD and realistic confining models

Motivation for relativistic models

Aspects of the Strong Interactions

The Chiral Confining model

The NJL chiral potential

LσM vs NJL chiral potential

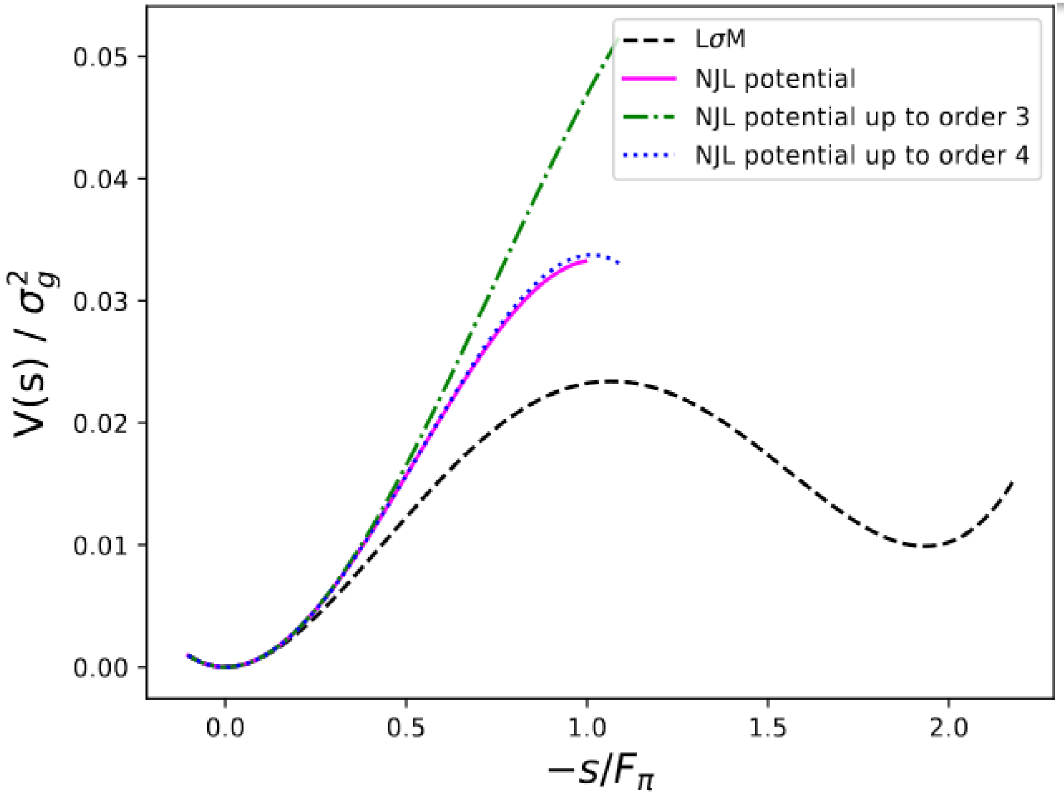

LσM

Simple and naive implementation of chiral symmetry
No links to the fundamental quark level whatsoever

$$V_{\chi,\mathrm{L\sigma M}}(s) = \frac{1}{2} m_s^2 s^2 + \frac{1}{2} \frac{m_s^2 - m_\pi^2}{F_\pi} s^3 + \frac{1}{8} \frac{m_s^2 - m_\pi^2}{F_\pi^2} s^4$$

NJL chiral potential

NJL model is specifically use to study chiral symmetry at the fundamental quark level

Provides a better description of the low energy realization of chiral symmetry in the hadronic sector

After linearisation:

$$V_{\chi,\mathrm{NJL}}(s) \approx \frac{1}{2} m_s^2 s^2 + \frac{1}{2} \frac{m_s^2 - m_\pi^2}{F_\pi} (1 - C_{\chi,\mathrm{NJL}}) s^3 + \ldots$$

a2 and a4 now become[1]:

$$a_2 = \frac{F_\pi \, g_S}{m_s^2} \qquad a_4 = -\frac{F_\pi \, g_S}{2 m_s^4} \left(3 - 2 \tilde{C}_L\right) \quad \text{with} \quad \tilde{C}_L = \frac{M_N}{g_S \, F_\pi} C + \frac{3}{2} C_\chi$$

[1] Chanfray, Hansen, Margueron, EPJA (2023)

Parameterisation

Parameters:

Tensor interaction coupling

- = 6.6 suggested by scattering data
- = 3.7 suggested by the Vector Dominance Model (VDM)

Vector interaction coupling

- Absence, i.e. =0

Constraints	centroid	std. dev. (or total width)
a_2 (GeV^{-1})	1.553	0.136★
a_4 (GeV^{-3})	-0.509	0.054★
F_π (MeV)	92	2
m_π (MeV)	139.6	2
M_0 (MeV)	$<$ 400 MeV	
$\Lambda^2 G_1$	5.5	9★
E_{sat} (MeV)	-15.8	0.3
n_{sat} (fm^{-3})	0.155	0.005
K_{sat} (MeV)	230	20

Bayesian analysis (G2 = 0)

Chamseddine, et al, EPJA60 (2024)

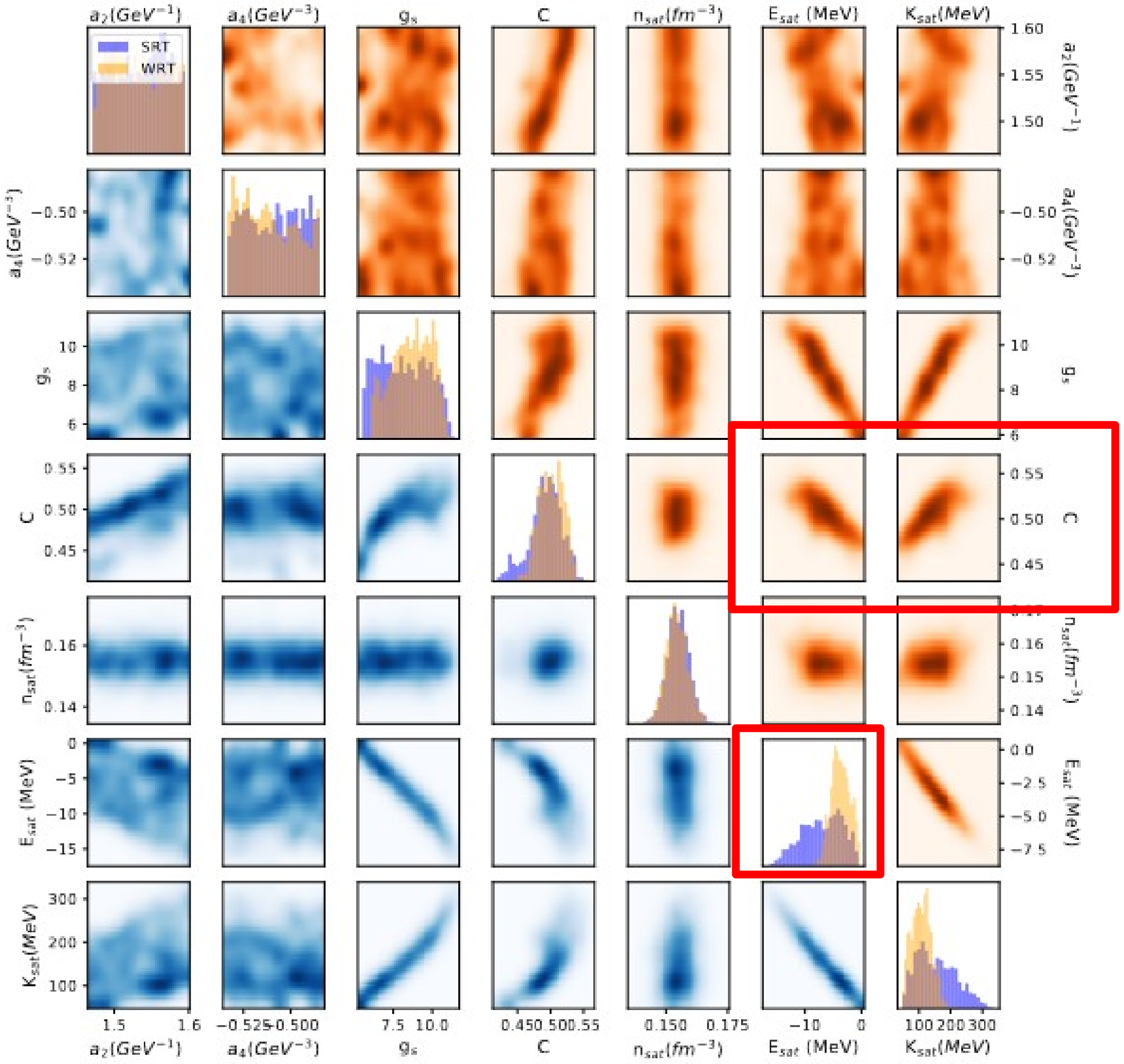

Bayesian analysis (G2 = G1)

Chamseddine, et al. EPJA60 (2024)

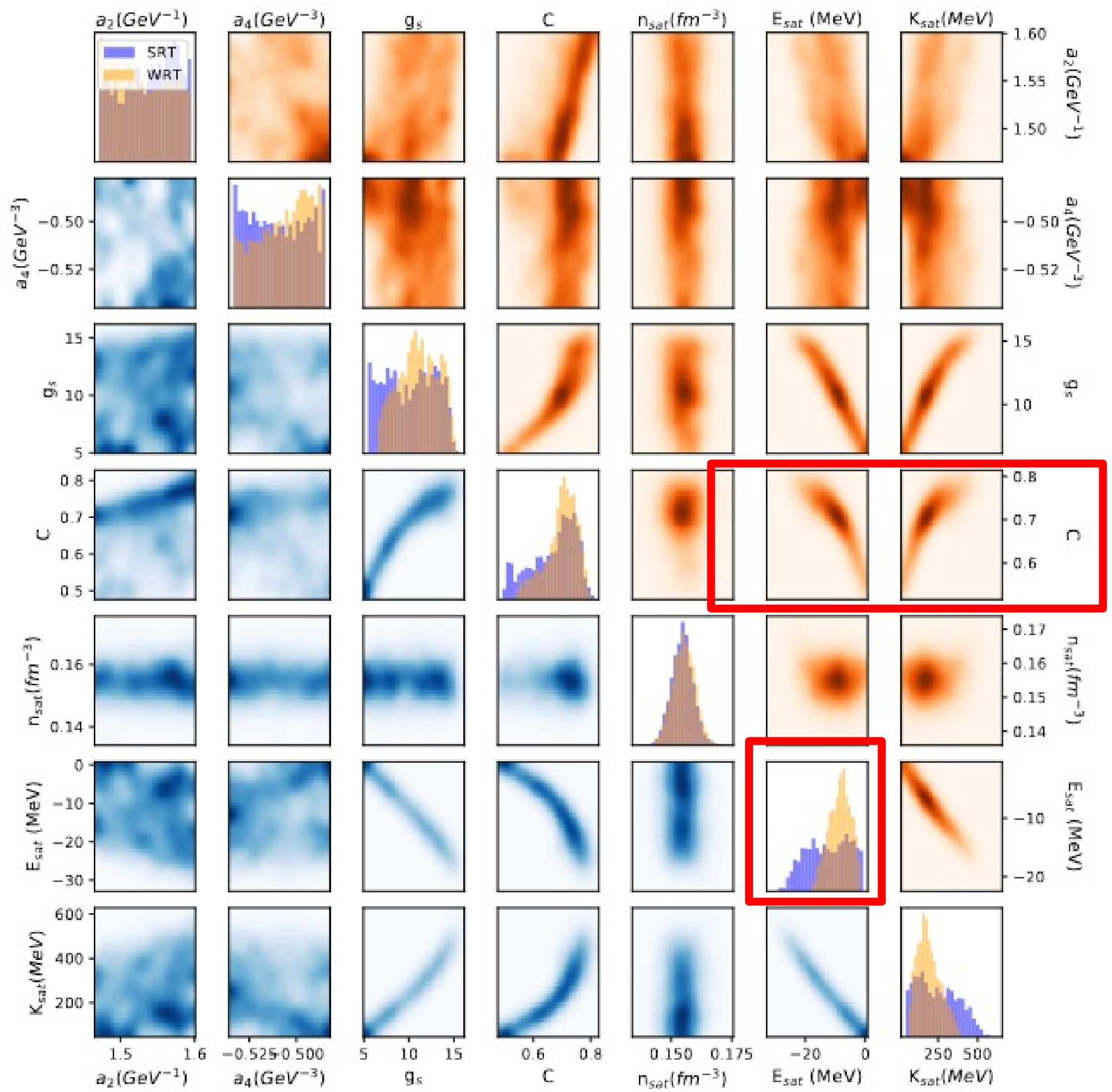

Breakdown density

Chamseddine, et al EPJA60 (2024)

- From the set of EoM, the following:

$$V'(\bar{s}) = -g_s^* n_s$$

stops having a solution once near the minimum of *V'(s)*

- The NJL potential being steeper, breaks down earlier than LσM (4-14 times n_{sat})

- The breakdown is purely of mathematical nature, no reason to assume phase transitions

- Limits the domain of applicability of the model in density

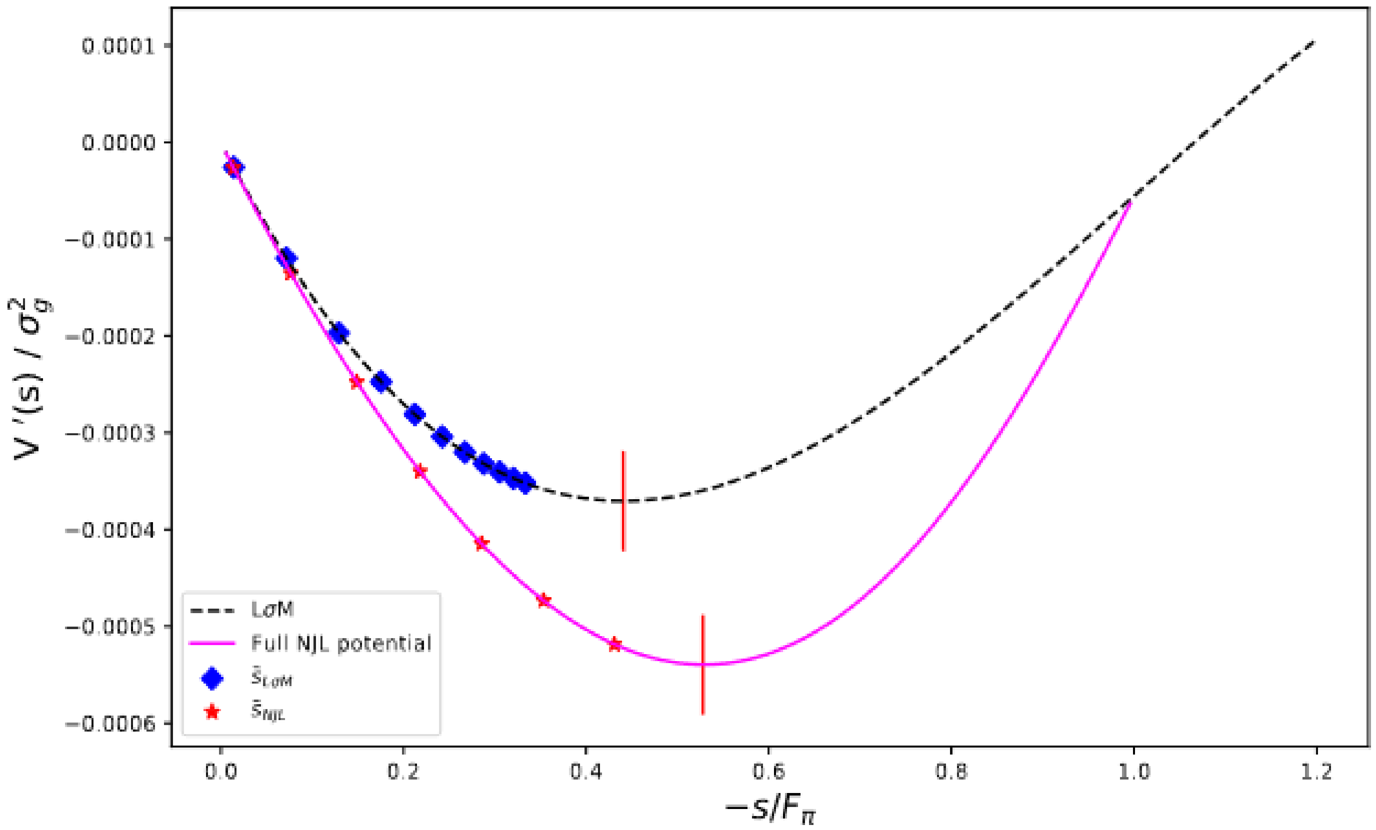

Key points

We use the NJL model to get a more realistic chiral potential

Tension between LQCD and realistic confining models is resolved

These models have a breakdown density of mathematical origin

Indication of a “missing” attractive energy which points towards pion loops corrections

Motivation for relativistic models

Aspects of the Strong Interactions

The Chiral Confining model

The NJL chiral potential

Finite nuclei

Spherical nuclei

- DIRHBS code (*Computer Physics Communications Volume 185, Issue 6, June 2014, Pages 1808-1821) T. Nikšić et al*

- Pairing is included (separable the Gogny force D1S)

- Hartree level only (direct terms)

- We tested the RMFCC model, and an additional similar model Parity Doublet Model (PDM)
  Eur. Phys. J. A (2023) 59:149 and *Phys. Rev. C 109, 045201*

Finite nuclei

Nucleus	Model	E_{tot} (MeV)	$E_{pairing}$(n/p) (MeV)	R_C (fm)
^{16}O	NL3	-126.83	0.0/0.0	2.726
	DD-ME2	-127.81	0.0/0.0	2.726
	PDM	-122.75	0.0/0.0	2.762
	RMFCC1	-128.44	0.0/0.0	2.706
	RMFCC2	-134.77	0.0/0.0	2.806
	Exp	-128.00	0.0/0.0	2.699
^{40}Ca	NL3	-341.07	0.0/0.0	3.470
	DD-ME2	-342.78	0.0/0.0	3.464
	PDM	-332.25	0.0/0.0	3.469
	RMFCC1	-344.36	0.0/0.0	3.428
	RMFCC2	-345.88	0.0/0.0	3.572
	Exp	-342.69	0.0/0.0	3.478
^{48}Ca	NL3	-414.76	0.0/0.0	3.471
	DD-ME2	-414.81	0.0/0.0	3.480
	PDM	-396.68	-21.65/0.0	3.531
	RMFCC1	-409.67	-22.05/0.0	3.500
	RMFCC2	-420.31	0.0/0.0	3.614
	Exp	-414.33	0.0/0.0	3.477
^{72}Ni	NL3	-613.78	-8.43/0.0	3.895
	DD-ME2	-612.69	-7.15/0.0	3.914
	PDM	-614.98	-15.43/-20.45	3.945
	RMFCC1	-611.90	-17.18/-22.63	3.934
	RMFCC2	-611.93	-9.01/0.0	4.074
	Exp	-613.173	-9.0/0.0	3.914*
^{90}Zr	NL3	-783.17	0.0/-8.40	4.265
	DD-ME2	-783.19	0.0/-5.55	4.268
	PDM	-778.30	-22.55/-5.35	4.281
	RMFCC1	-775.30	-25.42/-8.57	4.274
	RMFCC2	-776.03	0.0/-7.85	4.274
	Exp	-783.89	0.0/-8.0	4.272
^{116}Sn	NL3	-986.86	-14.15/0.0	4.609
	DD-ME2	-987.17	-9.43/0.0	4.615
	PDM	-990.74	-14.09/-23.76	4.630
	RMFCC1	-986.77	-15.59/-27.09	4.618
	RMFCC2	-975.39	-14.27/0.0	4.798
	Exp	-988.681	-17./0.0	4.626
^{124}Sn	NL3	-1049.42	-14.49/0.0	4.661
	DD-ME2	-1049.10	-11.17/0.0	4.671
	PDM	-1055.69	-19.31/-24.59	4.690
	RMFCC1	-1049.68	-22.50/-27.94	4.678
	RMFCC2	-1043.29	-15.79/0.0	4.854
	Exp	-1049.96	-15./0.0	4.674
^{132}Sn	NL3	-1104.32	0.0/0.0	4.710
	DD-ME2	-1103.60	0.0/0.0	4.718
	PDM	-1107.44	-25.02/-25.22	4.764
	RMFCC1	-1099.71	-28.94/-28.61	4.750
	RMFCC2	-1105.70	0.0/0.0	4.907
	Exp	-1102.860	0.0/0.0	4.718*
^{204}Pb	NL3	-1609.31	-7.17/0.0	5.499
	DD-ME2	-1608.94	-6.59/0.0	5.600
	PDM	-1619.57	-33.49/-33.07	5.535
	RMFCC1	-1608.76	-39.13/-37.87	5.518
	RMFCC2	-1587.67	-6.90/0.0	5.692
	Exp	-1607.520	-10./0.0	5.486
^{208}Pb	NL3	-1639.28	0.0/0.0	5.516
	DD-ME2	-1640.02	0.0/0.0	5.518
	PDM	-1651.08	-30.32/-33.64	5.561
	RMFCC1	-1639.44	-35.72/-38.41	5.544
	RMFCC2	-1619.85	0.0/0.0	5.708
	Exp	-1636.446	0.0/0.0	5.505

Parameters	m_s (MeV)	C	g_s	g_ω	g_ρ
FN + NEP	455.76	0.593	5.970	5.614	4.309
FN + SPE	685.15	0.891	13.760	13.122	3.781
FN + NEP + NP	682.13	0.841	12.690	11.890	3.820

Single Particle Energies

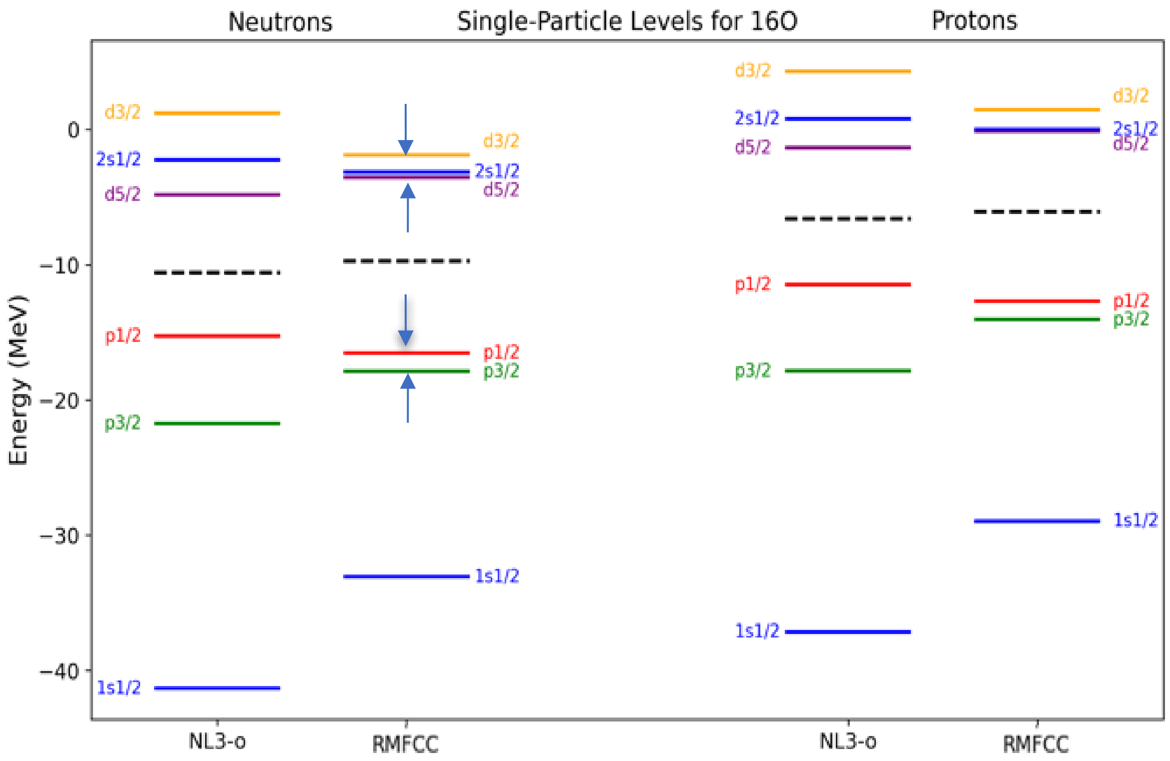

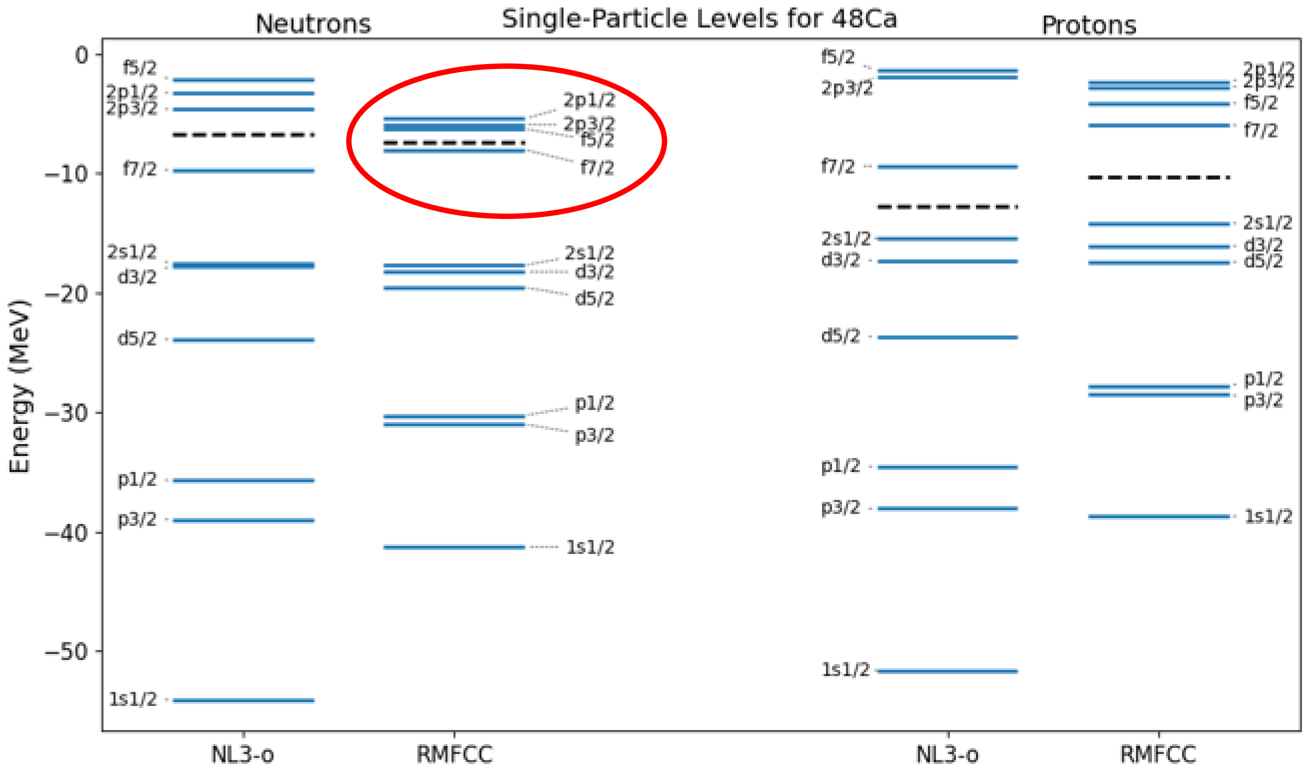

Motivation for relativistic models

Aspects of the Strong Interactions

The Chiral Confining model

The NJL chiral potential

Finite nuclei

Conclusions and outlooks

Conclusion

- We managed to propose a model with properties from QCD anchored at the fundamental level
- We resolved the tension that arose between LQCD and realistic confining models
- The model presents a breakdown density which would represent the maximal density for an EoS for neutron stars
- The model presents good predictions for nuclear structure (binding energies, charge radii,…) at the RMF level, however the spin-orbit potential is too weak which leads to uncorrect predicitons for SPE

Outlooks

- Exploring high densities by connecting the model to a quark phase via some phase transitions
- Including Fock terms, at the local approximation (or the heavy meson limit), and see whether it is capable of solving the single particle energies problem

Publications

1. Chamseddine, Margueron, Chanfray, Hansen, Somasundaram, Relativistic Hartree–Fock chiral Lagrangians with confinement, nucleon finite size and short-range effects. *EPJA, vol. 59, no. 8, Aug. 2024*

2. Chamseddine, Margueron, Hansen, Chanfray, Hartree-Fock Lagrangians with a Nambu-Jona–Lasino scalar potential. *EPJA, vol. 60, no. 6, p. 137, 2024*

THANK YOU !

Extra slides

Fitting data + results

Phys. Rev. C 71

Nucleus	BE (MeV)	r_c (fm)	$r_n - r_p$ (fm)	dE	dr_c	dr_{np}
^{16}O	127.801 (127.619)	2.727 (2.730)	−0.03	0.1	−0.1	
^{40}Ca	342.741 (342.052)	3.464 (3.485)	−0.05	0.2	−0.6	
^{48}Ca	414.770 (415.991)	3.481 (3.484)	0.18	−0.3	−0.1	
^{72}Ni	612.655 (613.173)	3.914	0.28	−0.1		
^{90}Zr	783.155 (783.893)	4.275 (4.272)	0.07	−0.1	0.1	
^{116}Sn	986.928 (988.681)	4.615 (4.626)	0.12 (0.12)	−0.2	−0.2	3.8
^{124}Sn	1048.859 (1049.962)	4.671 (4.674)	0.21 (0.19)	−0.1	−0.1	10.7
^{132}Sn	1103.469 (1102.860)	4.718	0.26	0.1		
^{204}Pb	1608.506 (1607.520)	5.500 (5.486)	0.17	0.1	0.3	
^{208}Pb	1638.426 (1636.446)	5.518 (5.505)	0.19 (0.20)	0.1	0.2	−4.7
^{214}Pb	1661.182 (1663.298)	5.568 (5.562)	0.24	−0.1	0.1	
^{210}Po	1649.695 (1645.228)	5.552	0.17	0.3		

Parameters	centroid	std. dev.
E_{sat} (MeV)	-16	5%
n_{sat} (fm^{-3})	0.16	10%
E_{sym} (MeV)	31	10%
K_{sat} (MeV)	250	10%

Fitting data + results

Phys. Rev. C 71

Nucleus	BE (MeV)	r_c (fm)	$r_n - r_p$ (fm)	dE	dr_c	dr_{np}
^{16}O	127.801 (127.619)	2.727 (2.730)	−0.03	0.1	−0.1	
^{40}Ca	342.741 (342.052)	3.464 (3.485)	−0.05	0.2	−0.6	
^{48}Ca	414.770 (415.991)	3.481 (3.484)	0.18	−0.3	−0.1	
^{72}Ni	612.655 (613.173)	3.914	0.28	−0.1		
^{90}Zr	783.155 (783.893)	4.275 (4.272)	0.07	−0.1	0.1	
^{116}Sn	986.928 (988.681)	4.615 (4.626)	0.12 (0.12)	−0.2	−0.2	3.8
^{124}Sn	1048.859 (1049.962)	4.671 (4.674)	0.21 (0.19)	−0.1	−0.1	10.7
^{132}Sn	1103.469 (1102.860)	4.718	0.26	0.1		
^{204}Pb	1608.506 (1607.520)	5.500 (5.486)	0.17	0.1	0.3	
^{208}Pb	1638.426 (1636.446)	5.518 (5.505)	0.19 (0.20)	0.1	0.2	−4.7
^{214}Pb	1661.182 (1663.298)	5.568 (5.562)	0.24	−0.1	0.1	
^{210}Po	1649.695 (1645.228)	5.552	0.17	0.3		

Parameters	centroid	std. dev.
E_{sat} (MeV)	-16	5%
n_{sat} (fm^{-3})	0.16	10%
E_{sym} (MeV)	31	10%
K$_{sat}$ (MeV)	250	10%

$$\begin{aligned}
\text{FN+NEP:}\quad & E_{\rm sat} = -16.4\ \text{MeV}, \quad n_{\rm sat} = 0.155\ \text{fm}^{-3}, \\
& E_{\rm sym} = 32.09\ \text{MeV}, \quad K_{\rm sat} = 256\ \text{MeV} \\
\text{FN+SPE:}\quad & E_{\rm sat} = -15.41\ \text{MeV}, \quad n_{\rm sat} = 0.139\ \text{fm}^{-3}, \\
& E_{\rm sym} = 30.42\ \text{MeV}, \quad K_{\rm sat} = 202.00\ \text{MeV} \\
\text{FN+NEP+NP:}\quad & E_{\rm sat} = -15.81\ \text{MeV}, \quad n_{\rm sat} = 0.157\ \text{fm}^{-3}, \\
& E_{\rm sym} = 33.19\ \text{MeV}, \quad K_{\rm sat} = 184.83\ \text{MeV}
\end{aligned}$$

Pairing

- Since the calculations involving the finite-range Gogny force in the pairing channel require considerable computational effort, a separable form of the Gogny force has been introduced for RHB calculations in spherical and deformed nuclei

- The force is separable in momentum space, and is com-pletely determined by two parameters that are adjusted to reproduce the pairing gap of the Gogny force in symmetric nuclear matter

- The two parameters G and a have been adjusted to reproduce the density dependence of the gap at the Fermi surface, calculated with a Gogny force (D1S parameterization)

$$\Delta(k) = -\int_0^\infty \frac{k'^2 dk'}{2\pi^2} \langle k|V^{^1S_0}|k'\rangle \frac{\Delta(k')}{2E(k')},$$

and the pairing force is separable in momentum space

$$\langle k|V^{^1S_0}|k'\rangle = -Gp(k)p(k').$$

HVH theorem at Hartree level

- To reduce the inconsistencies, we worked at the Hartree level for the energies and self-energies (no Fock contributions at all)
- The vertex corrections can be simulated by a fictitious scalar field in such a way as to locally satisfy the HVH theorem:

$$\Sigma_S(\mathrm{p}) = \Sigma_S^D + \Sigma_S^E(\mathrm{p}) + \Sigma_R + \Sigma_{corr}$$

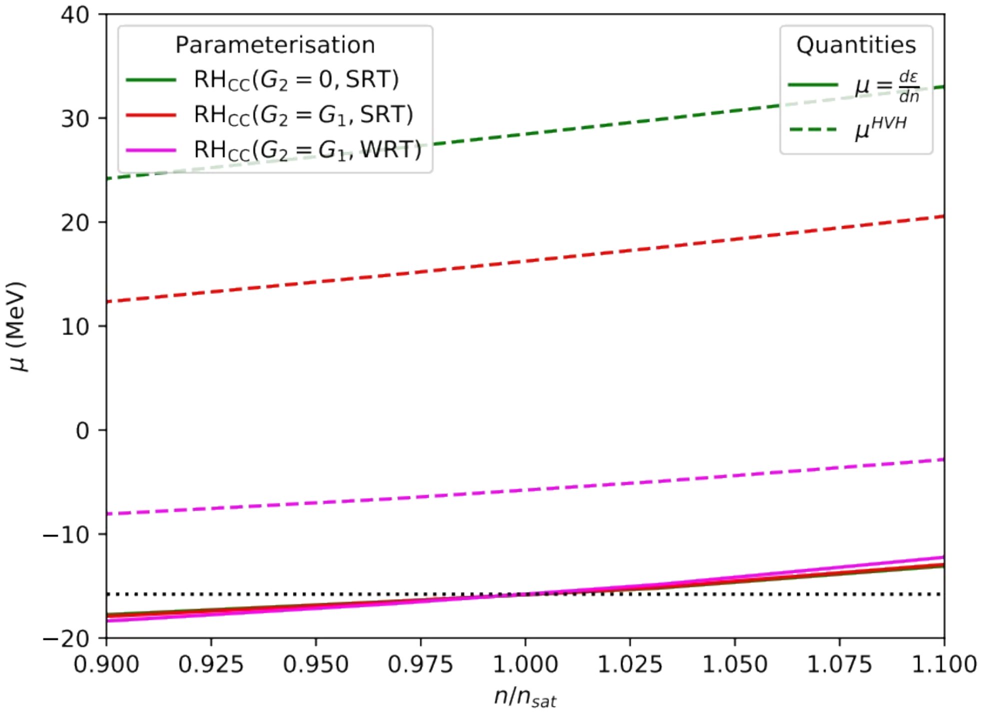

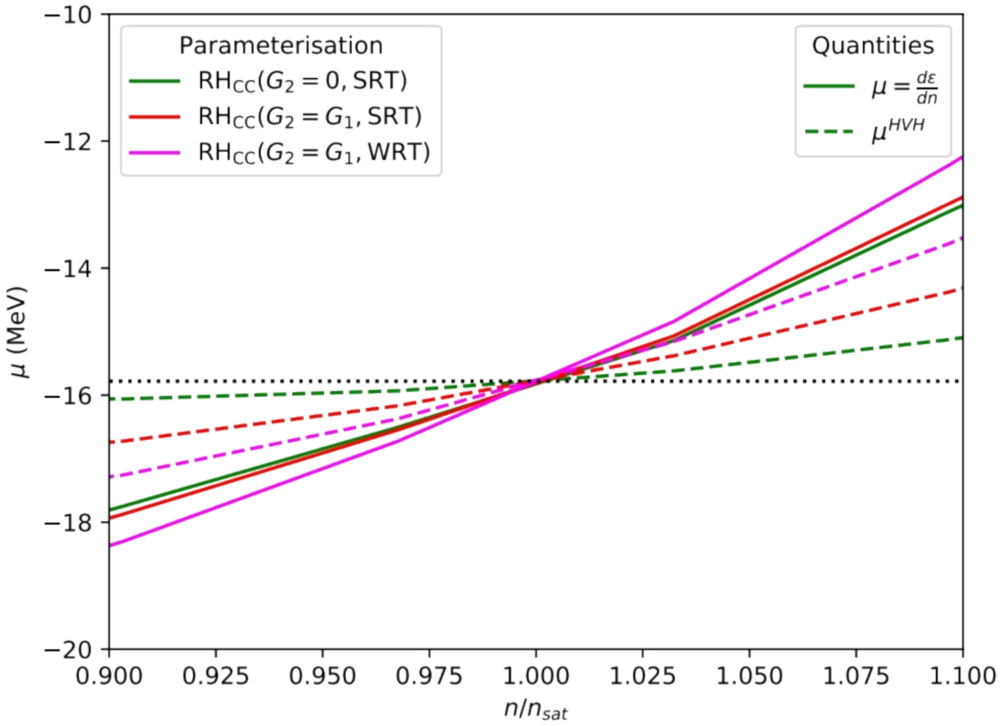

Pion condensation at Hartree level

No significant change in the onset of pion condensation, it is also triggered slightly earlier in density and isospin asymmetry

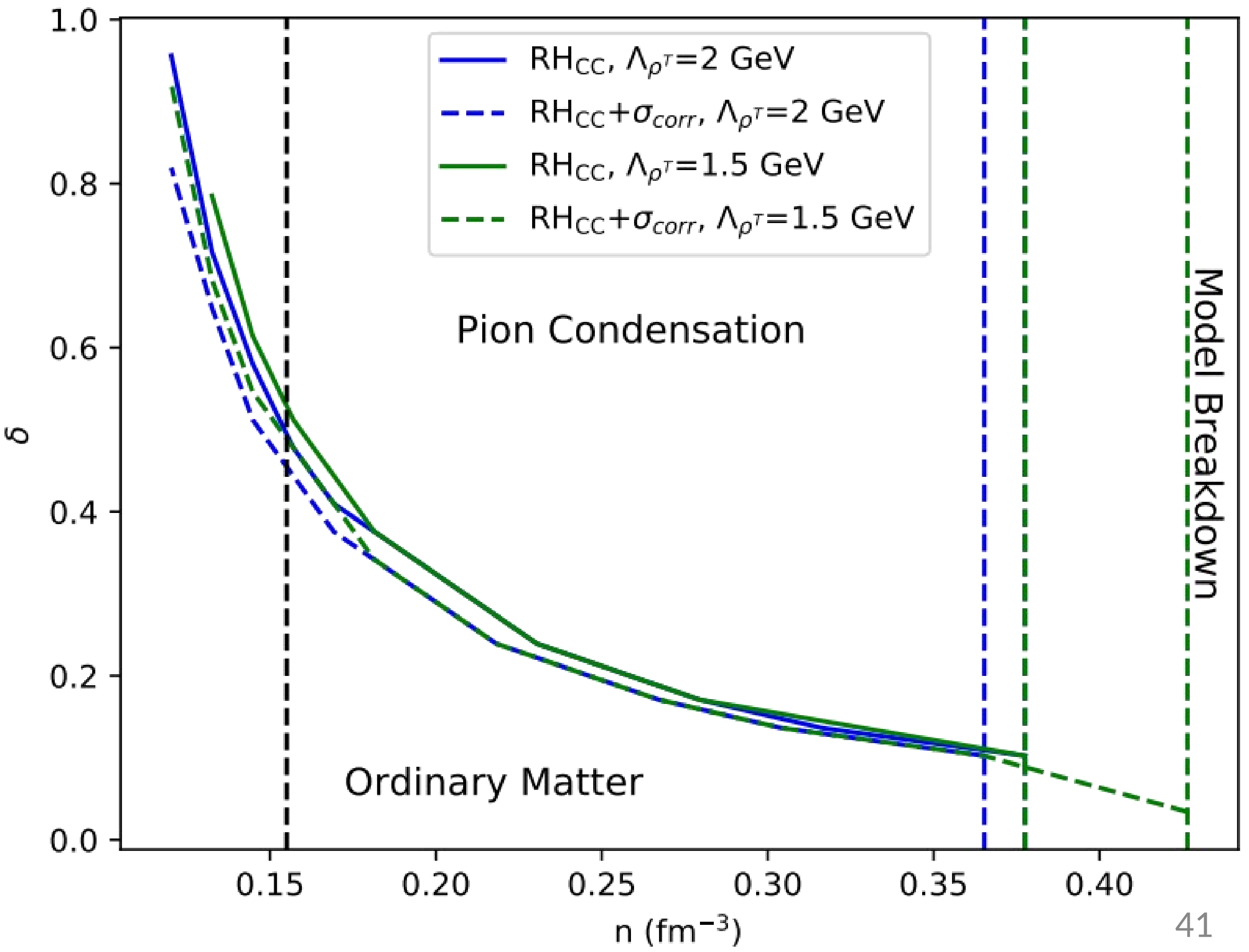

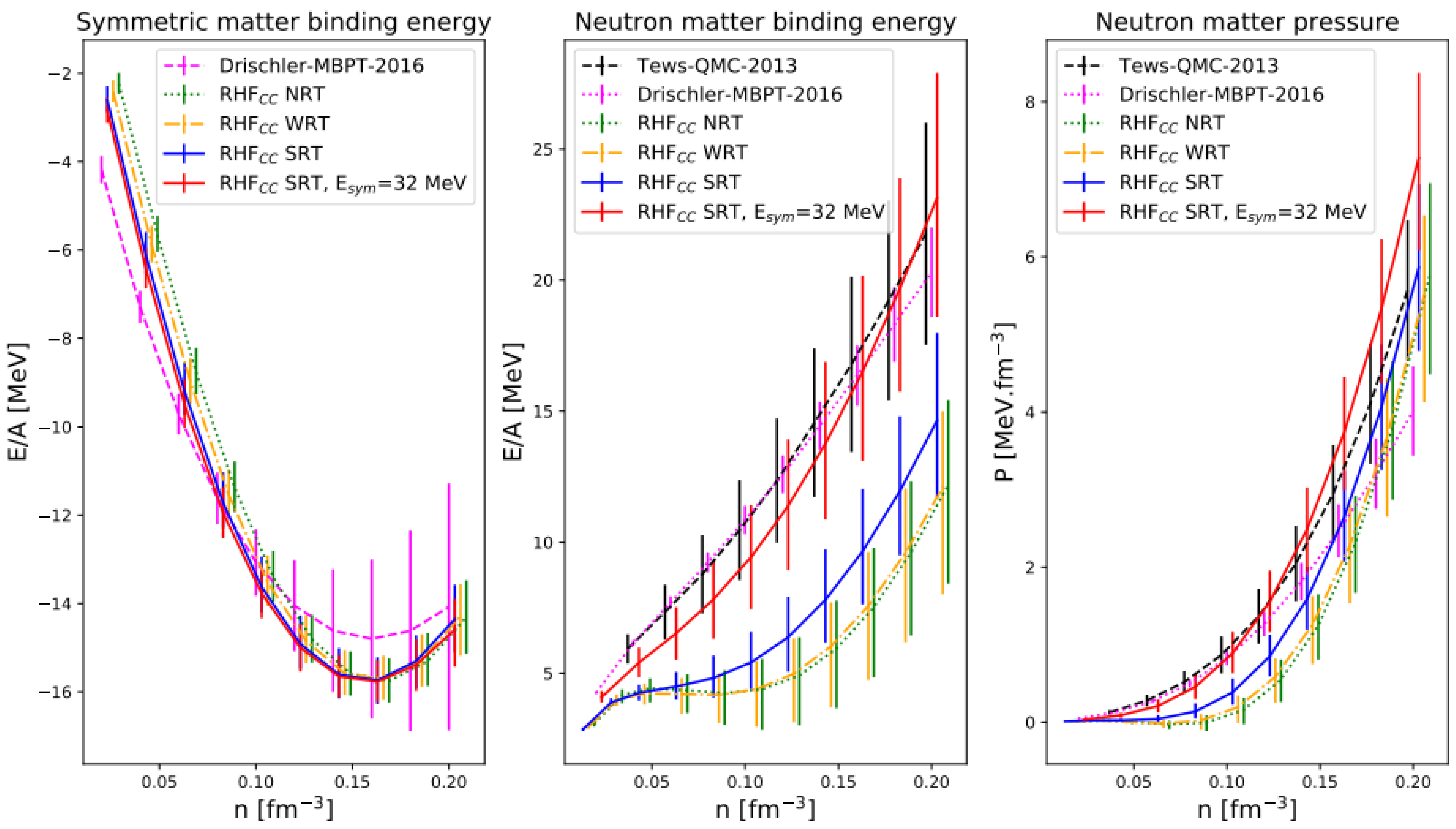
Symmetric matter binding energy
Drischler-MBPT-2016
RHF$_{CC}$ NRT
RHF$_{CC}$ WRT
RHF$_{CC}$ SRT
RHF$_{CC}$ SRT, E$_{sym}$=32 MeV
E/A [MeV]
n [fm^{-3}]
Neutron matter binding energy
Tews-QMC-2013
Drischler-MBPT-2016
RHF$_{CC}$ NRT
RHF$_{CC}$ WRT
RHF$_{CC}$ SRT
RHF$_{CC}$ SRT, E$_{sym}$=32 MeV
E/A [MeV]
n [fm^{-3}]
Neutron matter pressure
Tews-QMC-2013
Drischler-MBPT-2016
RHF$_{CC}$ NRT
RHF$_{CC}$ WRT
RHF$_{CC}$ SRT
RHF$_{CC}$ SRT, E$_{sym}$=32 MeV
P [MeV.fm^{-3}]
n [fm^{-3}]

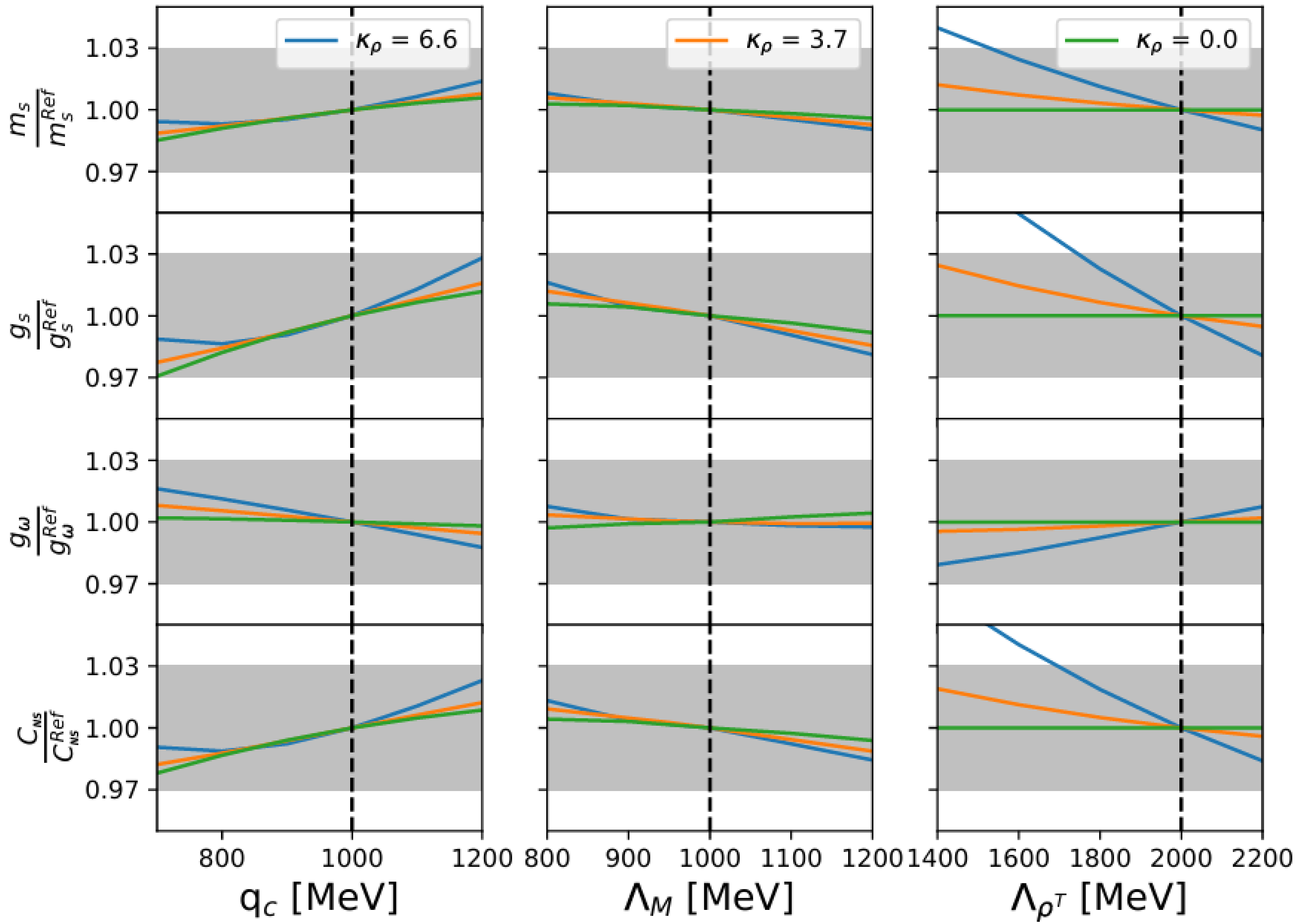

κ_ρ = 6.6
κ_ρ = 3.7
κ_ρ = 0.0
m_s / m_s^Ref
g_s / g_s^Ref
g_ω / g_ω^Ref
C_NS / C_NS^Ref
1.03
1.00
0.97
800
1000
1200
q_c [MeV]
800
900
1000
1100
1200
Λ_M [MeV]
1400
1600
1800
2000
2200
Λ_ρT [MeV]

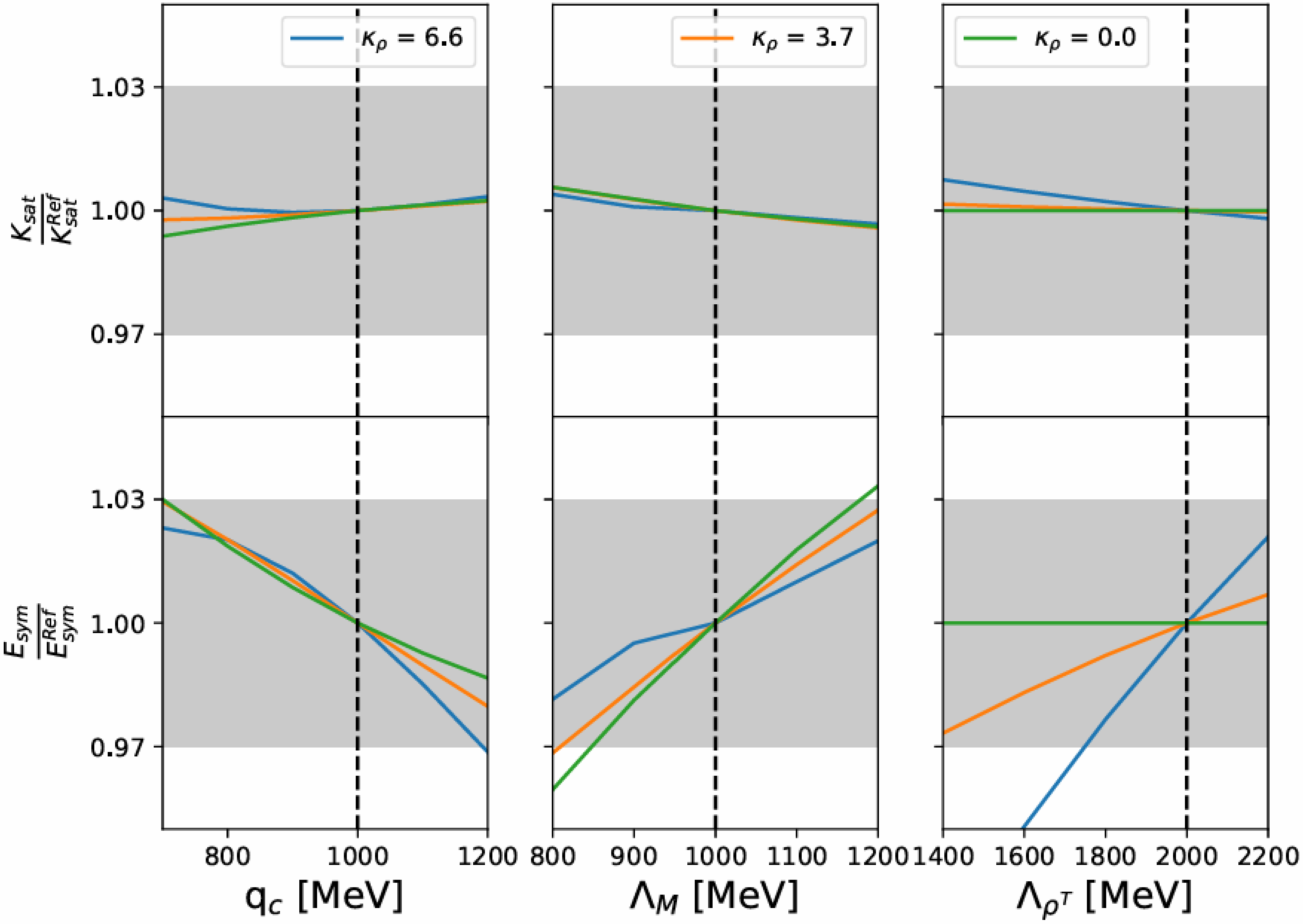

κ_ρ = 6.6
κ_ρ = 3.7
κ_ρ = 0.0
1.03
1.00
0.97
$\frac{K_{sat}}{K_{sat}^{Ref}}$
$\frac{E_{sym}}{E_{sym}^{Ref}}$
800
1000
1200
900
1100
1400
1600
1800
2000
2200
q_c [MeV]
Λ_M [MeV]
Λ_{ρ^T} [MeV]

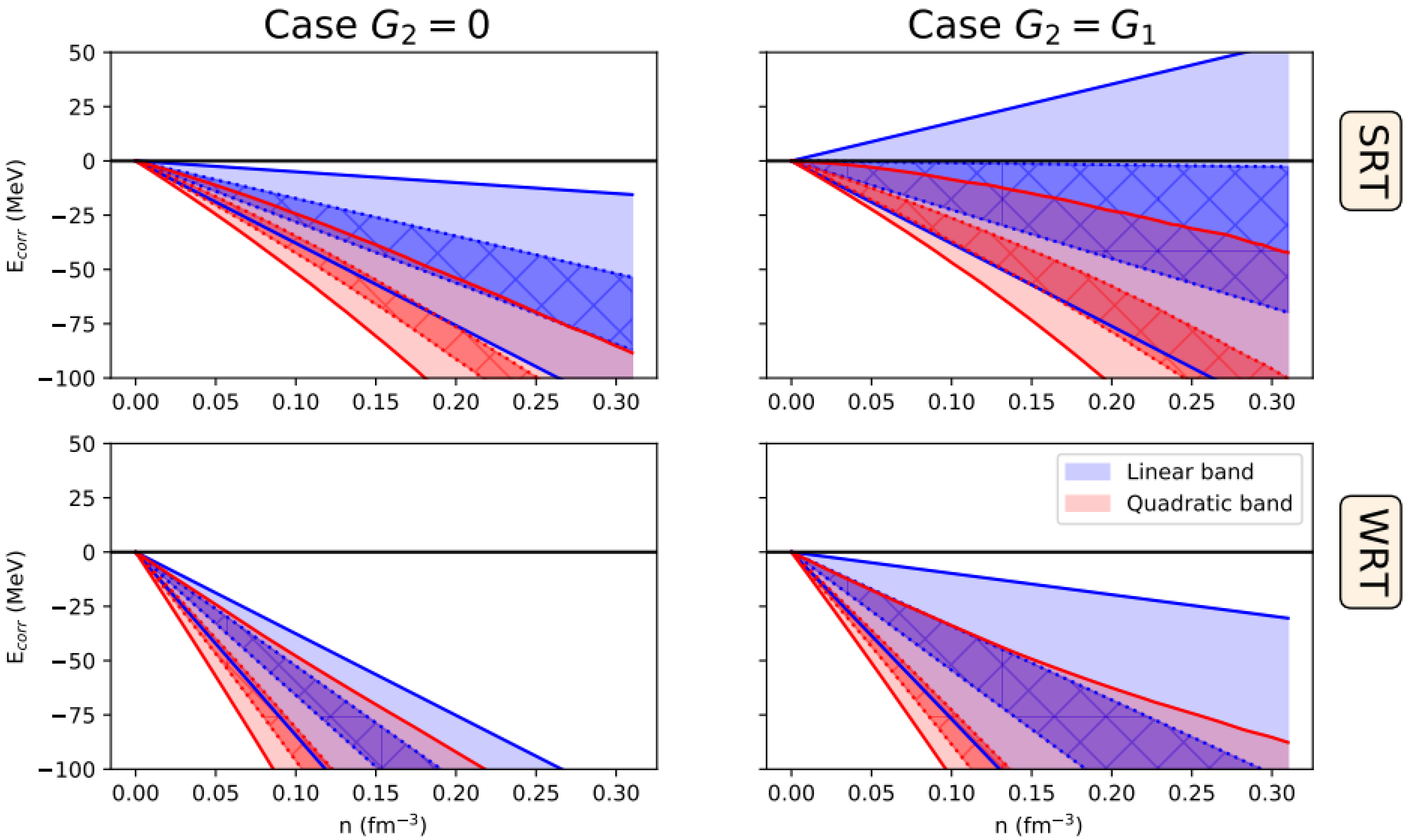
Case $G_2 = 0$
Case $G_2 = G_1$
SRT
WRT
E_{corr} (MeV)
n (fm^{-3})
Linear band
Quadratic band
50
25
0
−25
−50
−75
−100
0.00
0.05
0.10
0.15
0.20
0.25
0.30

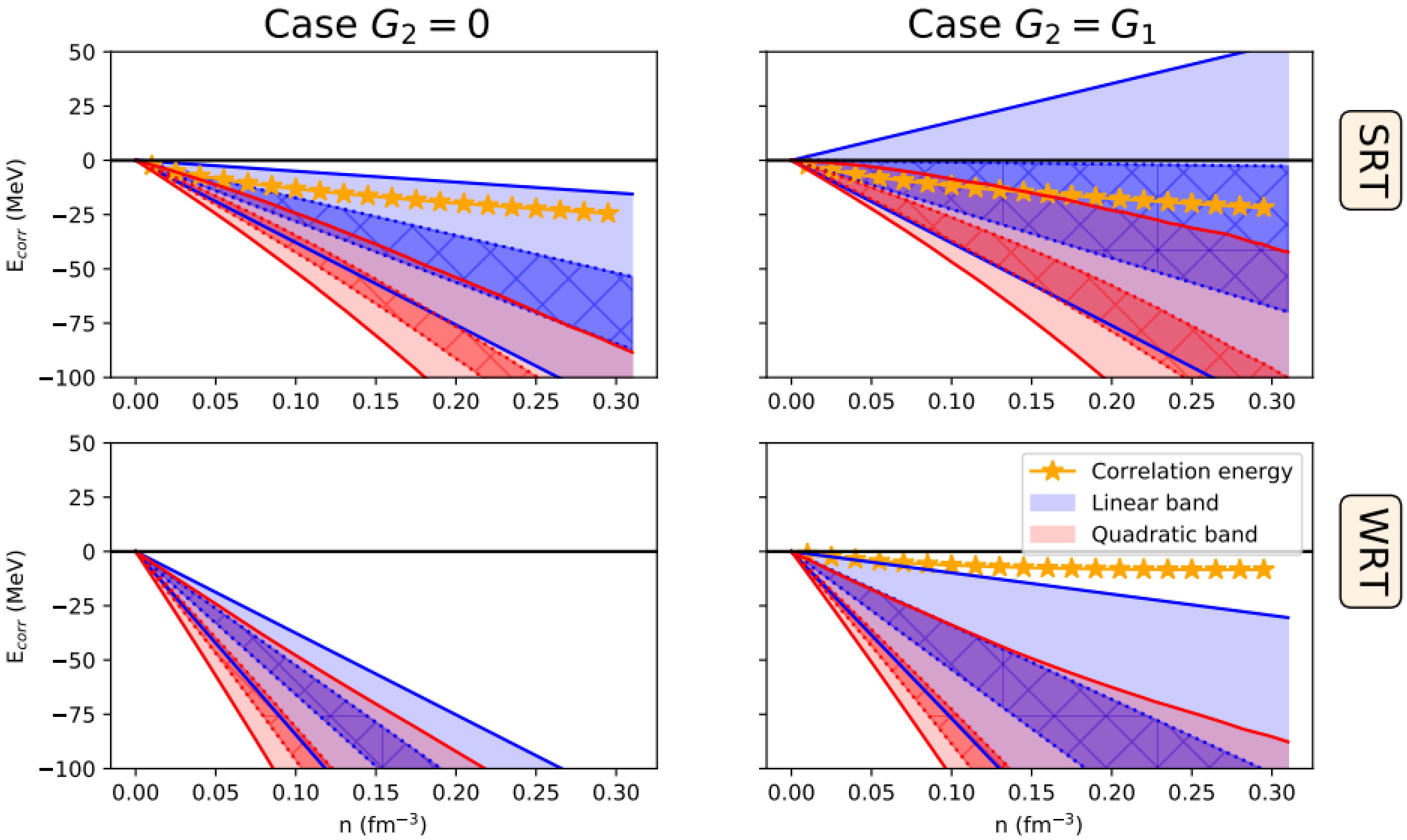

Case $G_2 = 0$
Case $G_2 = G_1$
SRT
WRT
E$_{corr}$ (MeV)
n (fm^{-3})
Correlation energy
Linear band
Quadratic band
50
25
0
−25
−50
−75
−100
0.00
0.05
0.10
0.15
0.20
0.25
0.30

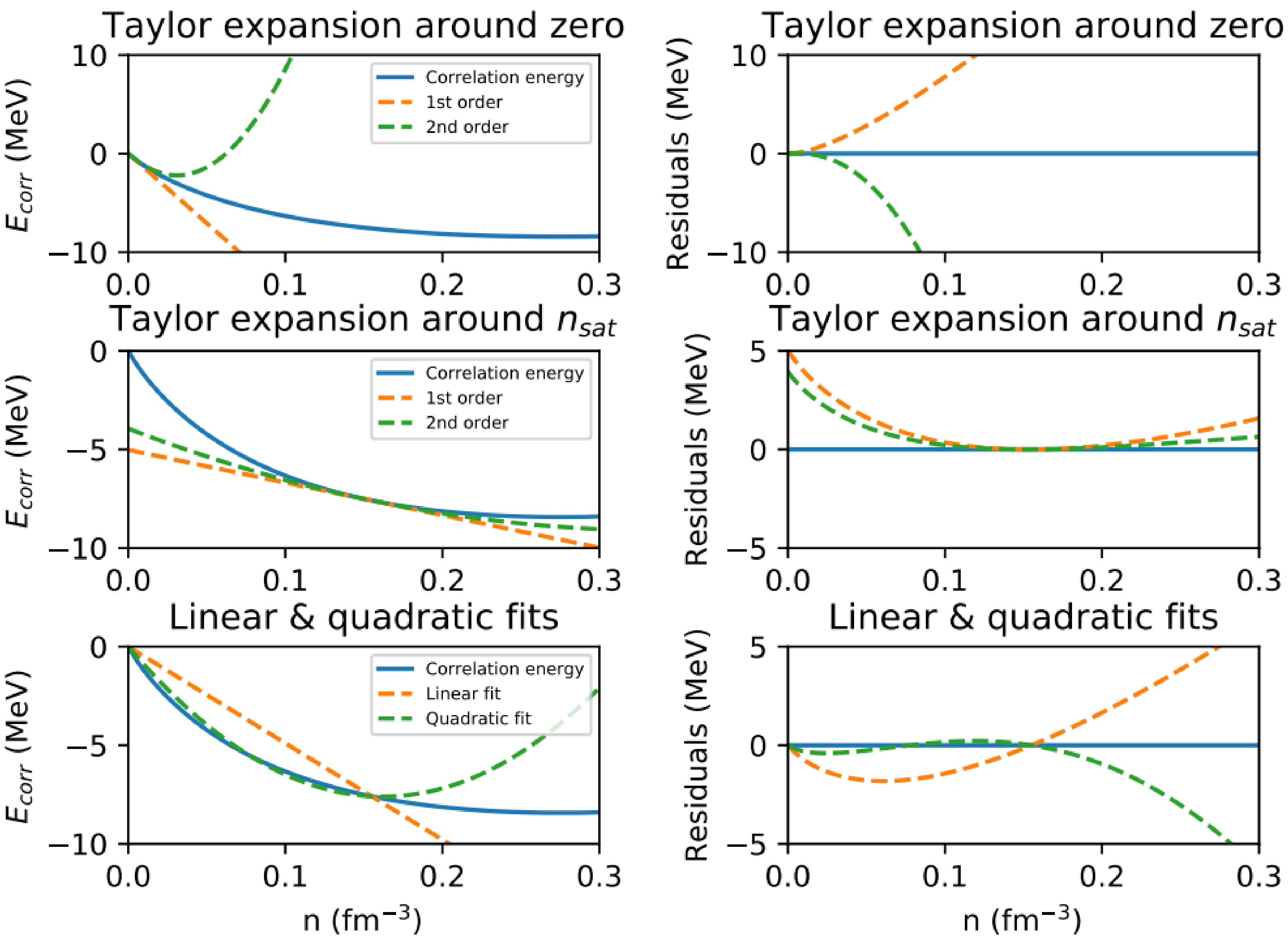

Taylor expansion around zero
Correlation energy
1st order
2nd order
E_{corr} (MeV)
Residuals (MeV)
Taylor expansion around n_{sat}
Linear & quadratic fits
Linear fit
Quadratic fit
n (fm^{-3})

$$
\begin{aligned}
V_{aL} &= \lambda^2 \left(\frac{g_A}{2\, f_\pi}\right)^2 \left(q^2 D_\pi(q) F_\pi^2(\mathbf{q}) - (g'_\pi - h'_\pi) + 3\frac{q^2}{\mathbf{q}^2} h'_\pi - (g'_\rho + 2h'_\rho)\right), \\
V_{aR} &= V_{aT} = -\lambda^2 \left(\frac{g_A}{2\, f_\pi}\right)^2 (g'_\pi - h'_\pi + g'_\rho + 2h'_\rho),
\end{aligned}
$$

$$
V_{\rho L} = V_{\rho R} = V_{\rho T} \equiv V_\rho = -\lambda^2\, g_\rho^2 \left(D_\rho(q) F_\rho^2(\mathbf{q}) - \frac{3}{C_\rho} \frac{h'_\rho}{\mathbf{q}}\right).
$$

The 2π exchange

- The π also plays a role in the intermediate range through 2π exchange (pion loop)

- It is usually simulated by a sigma meson, but since in our case this sigma meson is related to chiral symmetry, the pion loop needs to be incorporated explicitly

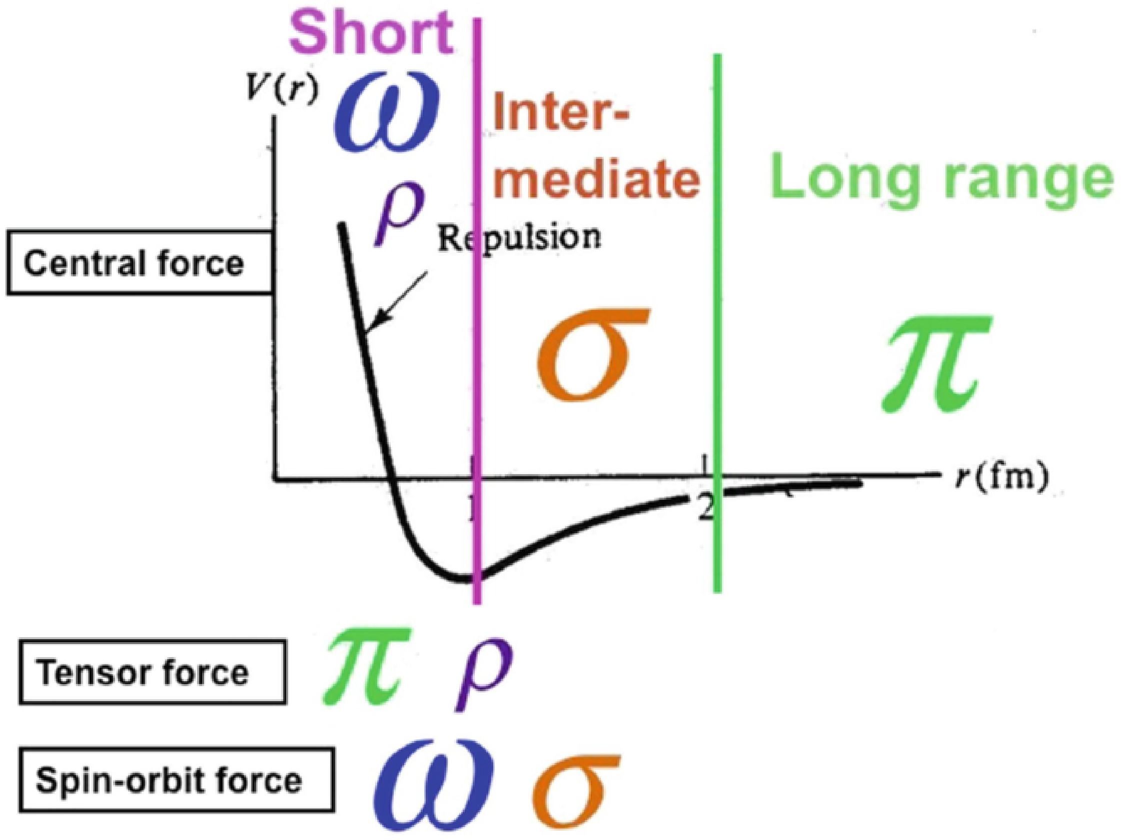

Approximations

1. The Fock terms introduce non-local effects for the Dirac mass and effective momentum, rendering the loop calculations extremely complicated

$$\mathbf{p}^* = \mathbf{p} + \tilde{\mathbf{p}}\Sigma_V(\mathrm{p})$$
$$M_D^*(\mathrm{p}) = M_N + \Sigma_S(\mathrm{p})$$

with

$$\Sigma_V(\mathrm{p}) = \Sigma \quad \mathrm{p})$$
$$\Sigma_S(\mathrm{p}) = \Sigma_S^D + \Sigma \quad \mathrm{p}) + \Sigma_R$$

We work in the Hartree basis in loops calculations, but we keep them for the Hartree-Fock energies

2. We have only included loops which contributes to the energy, but we have not added vertex corrections which should modify above equations

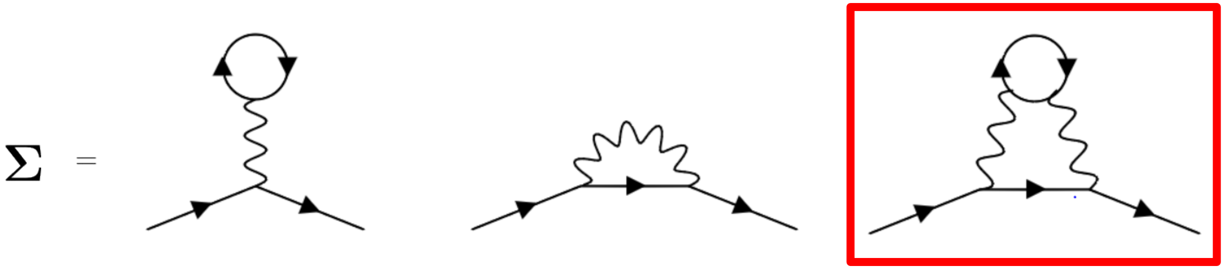

Results

Parameters						NEP			Correlation energies				
model	m	Λ	g_ω	G_1	C_{NS}	K_{sat}	$E_{\mathrm{sym},2}$	M_D^*/M_N	E_{aL}	E_{aR}	$E_{\rho R}$	E_T	E_{total}
	MeV	MeV		GeV^{-2}		MeV	MeV		MeV	MeV	MeV	MeV	MeV
$\mathrm{RHF}_{\mathrm{CC}}(G_2 = 0, \mathrm{WRT})$	-	-	-	-	-	-	-	-	-	-	-	-	-
$\mathrm{RHF}_{\mathrm{CC}}(G_2 = 0, \mathrm{SRT})$	5.62	619.95	7.716	11.466	0.504	194	28.1	0.80	-0.6	-0.0	-2.4	-14.0	-17
$\mathrm{RHF}_{\mathrm{CC}}(G_2 = G_1, \mathrm{WRT})$	3.47	743.64	8.832	7.763	0.743	251	31.2	0.72	-3.4	-0.0	-0.8	-3.4	-7.6
$\mathrm{RHF}_{\mathrm{CC}}(G_2 = G_1, \mathrm{SRT})$	3.33	802.35	7.451	6.115	0.634	201	26.7	0.81	-0.6	-0.0	-2.1	-12.5	-15.2

Pion condensation

- When we encounter a pole in the pion correlation function □ onset of pion condensation
- Highly dependent on the prescription and the cut-off
- Might be related to the inconsistent treatment

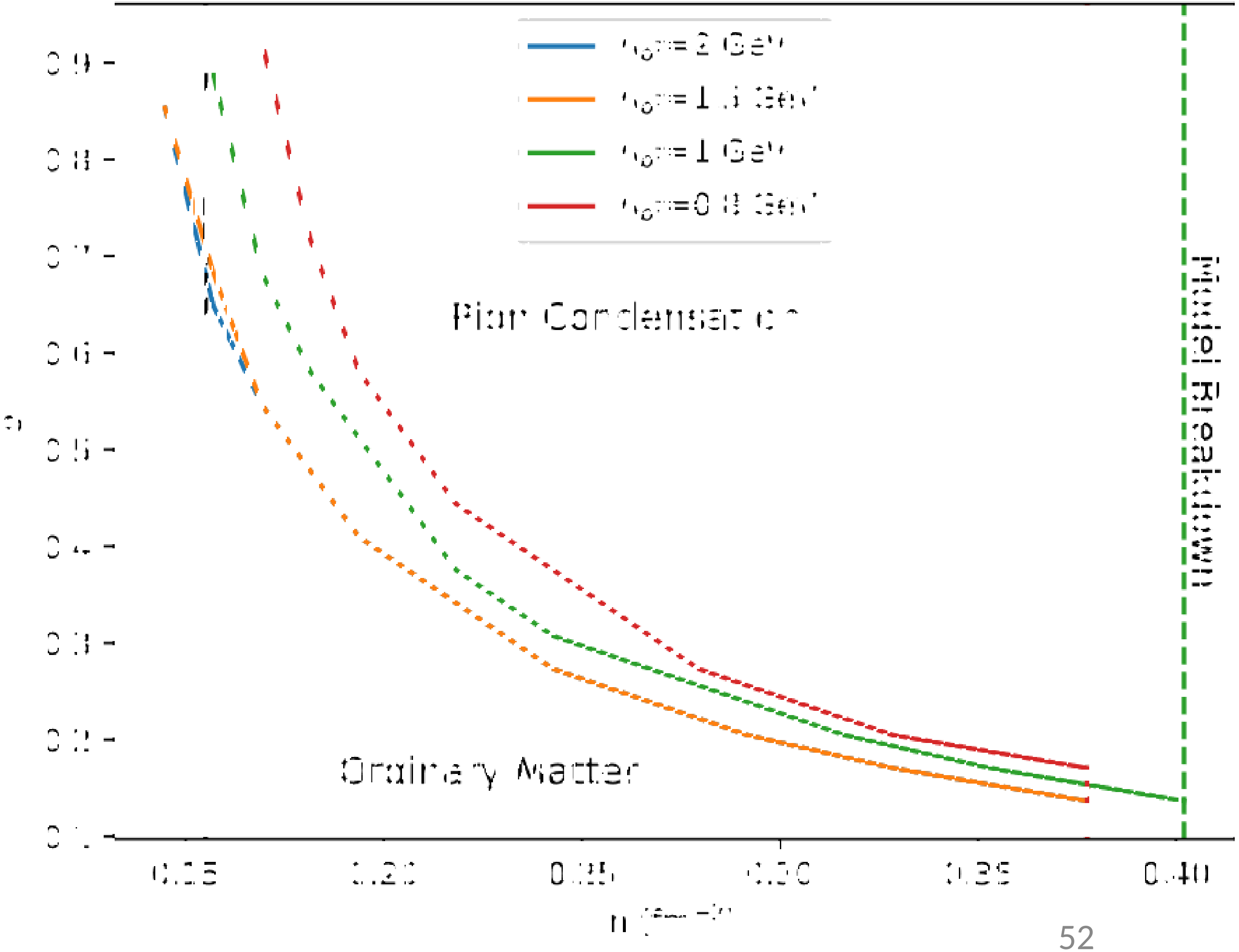

HVH theorem

- A thermodynamic test of the inconsistent approach

$$\mu^{HVH} = E^*(k_F) + \Sigma^0(k_F) = \left.\frac{d\epsilon}{dn}\right|_{n=n_{\rm sat}}$$

Microscopic definition (for $E^*(k_F) + \Sigma^0(k_F)$)

Thermodynamic definition (for $\left.\frac{d\epsilon}{dn}\right|_{n=n_{\rm sat}}$)

- We have an important violation of the theorem, which requires a more careful treatment in any future work

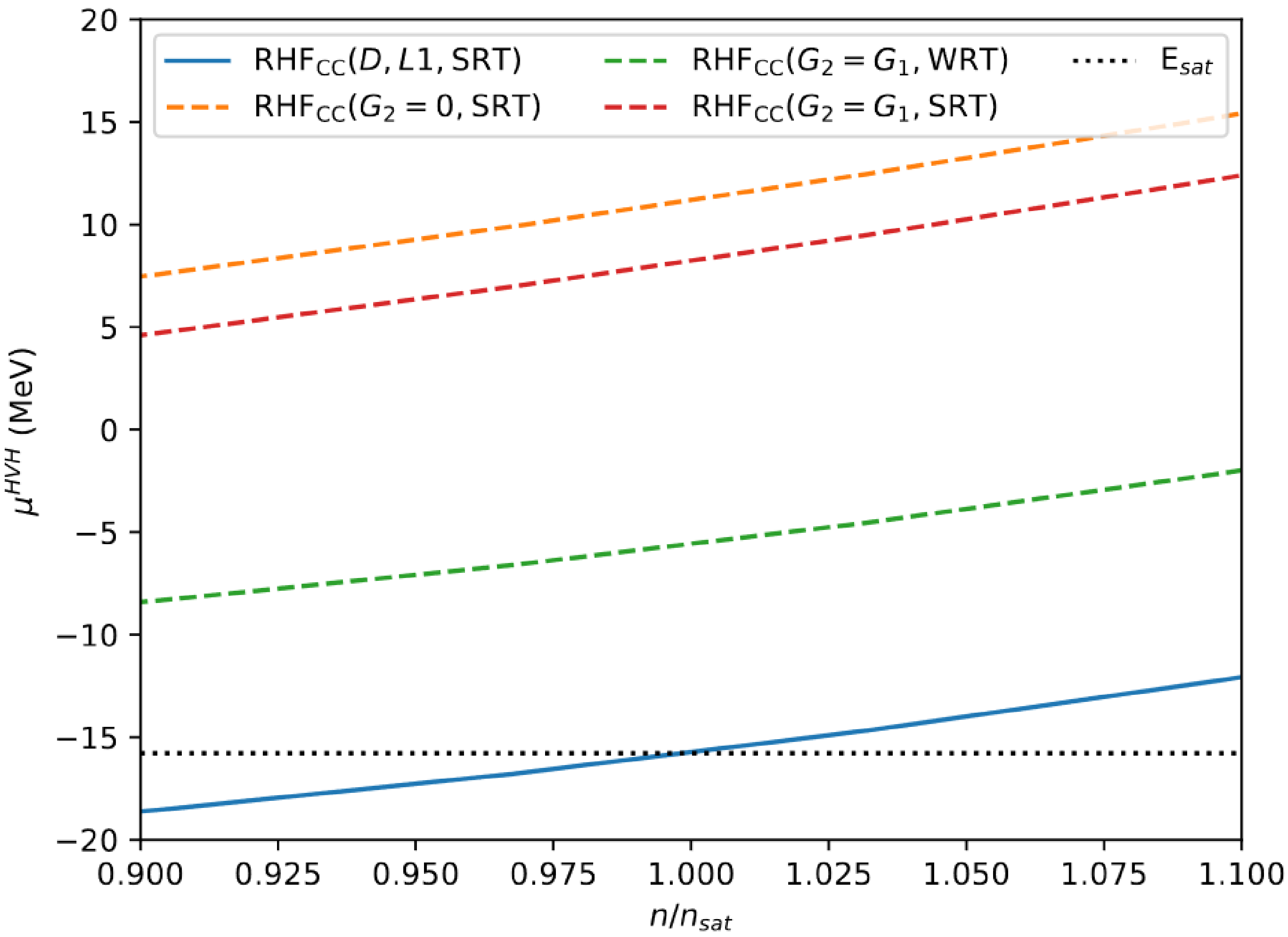

Key points

Pion loops corrections did solve (in most cases) the “missing” energy problem

Improvement of and in the right direction

Early onset of pion condensation dependent on the cut-off

Inconsistent treatment leads to an important violation of the HVH theorem can be reduced by a fictitious scalar field